Influence of Heat and Mass Transfer on the Performance of Large-Scale Thermal Energy Storage Systems

Alice Tosatto[1(✉)], Fabian Ochs[1], Abdulrahman Dahash[2], Christoph Muser[3], Felix Kutscha-Lissberg[4], and Peter Kremnitzer[4]

[1] Unit of Energy Efficient Building, University of Innsbruck, Innsbruck, Austria
alice.tosatto@uibk.ac.at
[2] Sustainable Thermal Energy Systems, Center for Energy, AIT Austrian Institute of Technology GmbH, Vienna, Austria
[3] Ste.p ZT-GmbH, Vienna, Austria
[4] PORR Bau GmbH, Vienna, Austria

Abstract. The current path towards the reduction of fossil-based energy carriers in District Heating systems involves an increasing use of renewable energy sources. In this perspective, the use of efficient thermal energy storage (TES) systems represents an important solution to allow a wider diversification and integration of renewable energy sources, which would otherwise be strongly limited. The use of large-scale buried TES (in particular pit TES) requires however a proper design, which takes into account both the TES operation characteristics and the envelope material properties. In particular, the TES envelope design requires a detailed study, considering its role in preserving the stored energy and the quality of surrounding groundwater. This study will focus on the thermal performance of the TES cover, being the most challenging envelope element. In order to gain detailed information regarding the behaviour of the insulation material in this specific application, it is necessary to investigate the effective materials properties in non-ideal conditions (i.e. moist conditions and high temperatures). The case study of foam glass gravel (FGG), an insulation material widely used in ground applications, is thereby presented to provide an exemplary overview of the challenges that can present in real operation conditions, such as the presence of residual moisture content from the construction phase and the development of convective heat (and mass) transfer. The analysis is supported by numerical simulations and experimental tests in order to investigate the influence of boundary conditions (i.e. heat flux direction, operation temperature, moisture content) and material configuration (i.e. compaction degree, thickness) on the effective insulation performance. Aim of the study is the definition of indications concerning the application of porous insulation materials in TES envelope, considering the challenges and the possible solutions.

Keywords: Thermal Energy Storage · thermal insulation · thermal conductivity · convection · moisture · performance · design

P. Schossig et al. (Eds.): IRES 2022, AHE 16, pp. 470–488, 2023.
https://doi.org/10.2991/978-94-6463-156-2_30

1 Introduction

Energy storage systems are a key element in the future energy system based on volatile and fluctuating renewable energy sources [1]. The increasing prices of fossil-based sources is pushing for a better exploit of the large amount of available renewable energy sources, thus requiring the development of efficient storage systems considering their fluctuating behaviour. Thermal energy storage (TES) systems are currently the most cost-effective solution in large-scale systems, such as district heating (DH) networks, thanks to the experience gained in the past decades (the first pilot solar DH plant with large-scale storage in Sweden dates back to 1979 [2]) and developments in recent years in Denmark, Germany and northern Europe, while integrations of TES in other countries such as Austria and China are currently under study [3].

The recently built TES systems in Denmark, in particular, represent the basis for the further improvement of this technology. Having now at least a decade of operation on their side, they are an important source of monitoring data, which can provide useful information about the TES performance in terms of achievement of the design targets (i.e. solar fraction), thermal stratification and eventually construction materials' problems [4].

Marstal TES and Dronninglund TES are two of the most important systems currently in use. The first, which went into operation in June 2012, shows a poorer performance with respect to the latter, in operation since March 2014. Despite the differences in construction (i.e. volume, lid liner and diffuser) and operation (Marstal has a seasonal operation, while Dronninglund has a combined seasonal and short-term operation), the seasonal efficiency was found to be a suitable indicator to compare their performance. In particular, Dronninglund TES had a 92% energy efficiency (average 2014–2019), while Marstal TES a 63% (average 2014–2017) [5]. The reason for this discrepancy was mainly due to the high thermal losses from the cover of Marstal, whose lid insulation showed a rapid degradation and was for this reason replaced in 2018.

The importance of the role played by large-scale TES systems is underlined by the high investments in this direction and by the number of projects that pursued the definition of optimal guidelines for their construction. In Austria the gigaTES project [6] worked to open the path for integrating large-scale buried TES systems in the Austrian context, considering the local DH features and land characteristics.

While the integration of the TES in the energy systems can be effectively planned with a proper energy management strategy, the construction and optimization of the TES itself remains a critical point. The influence of high temperature differences and moisture penetration on the performance and degradation of TES construction materials cannot be neglected in the planning phase. Construction guidelines able to address the local soil characteristics and TES design are therefore necessary to facilitate the planning process.

2 TES Envelope Requiremnets

2.1 Construction Challenges

One of the main challenges for the integration of large-scale TES in the energy systems is the effective design of the envelope, being it one of the main cost items and having a key impact on the component efficiency.

Currently, the main challenges faced in existing TES systems are:

-*High construction costs*. The current specific construction costs are around 30 €/m^3 for 'Danish pit' large scale TES [7]. However, when considering the necessity to access the cover surface (i.e. with a trafficable cover) these costs significantly increase. The construction of a tank TES, although more efficient to reduce the land use thanks to the more compact shape and higher depth, requires the application of special geotechnical works such as diaphragm walls, retaining anchors and protective groundwater measures [6]. The installation of lateral thermal insulation, required in presence of groundwater, is another important cost item, which adds up to ca. 300 €/$m^3{}_{ins}$. The development of cost-effective insulation solutions [8] is therefore a key element to reduce the investment costs.

-*Liner durability*. The selection of the liner material depends on the applied range of temperatures: polymer liners are applicable to low temperature systems, but, because of their fast degradation in contact with high temperatures, stainless steel (VA) liners are recommended in high temperature systems [9]. Among polymer liners, polypropylene (PP) and polyethylene (PE) are the most commonly used in the excavated pit TES (Marstal, Dronninglund, Chemnitz, Eggenstein-Leopoldshafen), while stainless steel liners are mainly used for tank TES (Rottweil, Friedrichshafen, Munich) [10]. The high cost difference between the two (50 €/m^3 for polymer liner against 150–300 €/m^3 for the VA liner [11]) make the first more competitive, provided that they are able to maintain a long-term stability against thermo-oxidation for at least 15–20 years of TES operation. When considering the most suitable material, its water vapor resistance should be considered, since water infiltrations in the envelope from the TES or from the surroundings (rainfall, groundwater) are not desirable, leading to a faster degradation of the insulation and of the liner itself.

-*Envelope performance*. As in the exemplary case of Marstal, a poor envelope quality led to a poor performance of the TES and accordingly of the DH network (low solar fraction) and required high maintenance effort, considering both the installation of the new lid and the lost operational period [10]. The cover represents a critical element in the TES as it is the envelope element with the highest specific thermal losses being exposed to the external air and different atmospheric conditions. These points make it necessary to use a material that combines high thermal performance, slow degradation and high-water vapor diffusion. In general, the presence of moisture in insulation materials negatively affects their performance as proven by several studies on building insulation materials and specific TES insulation materials [10]. A residual moisture content from the construction phase (e.g. from rainfall) should be avoided or removed.

-*Stratification decay*. The high thermal losses from the TES walls and cover lead to a fast decay of the natural thermal stratification, which is an important indicator of the TES performance [12]. However, the maintenance of this stratification is critical also during the mixing induced during charging and discharging phases. The optimal TES design (i.e. aspect ratio [13]) and location of the diffusers must minimize the temperature exchange within the TES height.

Altogether, these challenges contribute in preventing the reach of the design targets (i.e. efficiency, solar factor) and increase the return on investment period and the levelized cost of stored heat (LCOS) [13].

2.2 Degradation of TES Envelope Insulation

High temperature differences between the storage water and the outside ambient conditions result in high thermal losses, that affect both the TES performance and quality of the local ground conditions [14]. In tank TES systems, the sidewalls insulation might be therefore often necessary to comply with the local regulations, but its installation requires the use of scaffoldings. Instead, in many existing buried TES systems, the cover is the only insulated envelope element [12], since it is in contact with the upper hot water layers (at almost 90 °C in a high temperature storage) and the external air (which can reach temperatures well below 0 °C in winter in Austria).

Granular bulk insulation is a suitable material that can be applied as TES insulation, thanks to the ease of installation (the grains can be poured and adjusted to any geometrical irregularity). Foam Glass Gravel (FGG) is an interesting candidate, already widely employed in existing TES systems (e.g. Munich -Ackermannbogen, Eggenstein-Leopoldshafen [15]). Other suitable materials are perlite, expanded clay (EC) and expanded glass granules (ECG) [10]. As pointed out in [10], however, when comparing the design or simulation performance of existing TES with actual measurement data once in operation, the actual thermal losses are 30% to 50% higher. In the absence of failures or changes of the operating conditions, the main reason for this discrepancy is the over-optimistic thermal conductivity assumed during the design phase. The high temperatures involved, the insulation thickness and the presence of moisture are the main contributors to the poor insulation performance.

The use of a highly porous bulk is detrimental from the point of view of the insulation performance in presence of an upwards heat flux (as in the TES cover), since it could lead to the formation of natural convective transfer (that naturally establishes thanks to the air density gradient), that represents a non-negligible part of the total heat flux. Bianchi Janetti et al. [16] showed that, for upward heat flux and temperature differences higher than 10 K, the thermal conductivity of uncompacted bulk materials drastically deviates from the nominal values because of this convective component. In order to reduce this phenomenon, the material compaction is commonly used to reduce the bulk porosity and block the convective heat transfer. However, there is a lack of literature providing an analysis of the impact of large temperature differences in compacted porous media, which is the case of the TES cover. Moreover, a high compaction degree requires the use of a larger amount of material as well as time-consuming installation procedures. Therefore, the actual application in real TES systems requires a detailed analysis of the involved mechanisms. Additionally, increasing moisture content contributes in increasing the effective thermal conductivity of the material, since the moisture transport contributes in enhancing the heat transfer.

Overall, the sources of degradation of a buried TES envelope are mainly linked to moisture penetration and convection. Moisture penetration represents an important issue in the performance of the TES cover and can occur in the following ways:

1. Failure during construction (i.e. liner welding).
2. Diffusion from storage water through the liner or through leakages.
3. Moisture penetration from snow and rain linked to a poor component design, which does not allow the water run-off.

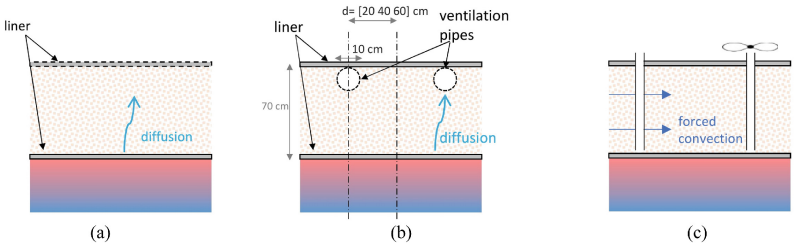

Fig. 1. Example of cover insulation solution with permeable liner (a), with ventilation pipes (b) and with forced convection (c).

4. Construction moisture, associated to the construction phase. As the size of the system forces operators to build on-site, the ambient weather conditions can affect the outcome. Unfavourable weather during the transport and installation of material leads to moist insulation.
5. Air bubbles in case of floating insulation cause an uneven surface in contact with the water.

Construction moisture does not depend on the design quality or the skills of the installators and can often be unavoidable on the construction side. It is however possible to implement solutions to get rid of both construction moisture and of the eventual moisture that diffuses through the liner in contact with the high temperature water. For what concerns the TES cover, the following mechanisms to avoid moisture accumulation can be used:

– diffusion: using a permeable upper liner (water tight to avoid rainfall water penetration, Fig. 1a) or ventilation pipes installed in the insulation layer (see Fig. 1b), thus relying on the diffusion of the water vapour.
– (forced) ventilation through the insulation layer: where convection is the main mechanism for heat and mass transfer (see Fig. 1c).

For what concerns the measures to avoid moisture accumulation in the cover, the solution of the ventilation pipes is presented in the following sections, since convection is generally not desirable in an insulation layer as it would enhance the heat transfer and thus the thermal losses.

3 Aim of the Work

The development of reliable and cost-effective insulation solutions is a key aspect to reduce the LCOS of a TES and to make this technology competitive in the energy transition. It is noteworthy to mention that there is no direct experience on the installation of sidewalls insulation in buried TES; its application in case of deep tank TES systems is however recommended in presence of groundwater [14]. Whereas in existing buried TES systems, cover thermal insulation is a key element; it is therefore going to be the focus of this work, being the element where the performance improvement margins are higher.

This work investigates the two sources of insulation degradation (moisture and convection) and the solutions applicable to reduce their impact on the cover insulation. The analysis is conducted with the help of numerical simulations, in order to investigate the influence of construction moisture in the cover on the total heat transfer and the possible solutions to remove it. Then, the influence of convection is investigated with an experimental set-up to examine its impact on the heat and moisture transfer in a porous insulation layer.

4 Heat and Moisture Transport in Porous Media

In solid materials, heat transfer is related to the conductive transfer, driven by the temperature difference, and by the latent heat of the evaporating water (Eq. (1)).

$$\left(\rho c_p\right)_{eq} \frac{\partial T}{\partial t} = \nabla \cdot \left(\lambda_{eq} \nabla T\right) + \nabla \cdot \left(L_v \left(\frac{D_{av}}{RT\mu}\right) \nabla (\varphi p_{sat})\right) \tag{1}$$

The moisture transport is driven by concentration gradients, as from Eq. (2). It is assumed that no capillary water transport occurs through the material.

$$\frac{\partial w}{\partial t} = -\nabla \cdot \left(-\frac{D_{av}}{RT\mu} \nabla (\varphi p_{sat})\right) \tag{2}$$

In presence of porosity, however, both heat and moisture transport are enhanced by the air and moisture fluxes driven by the fluid density gradients, that establish a free (or natural) convective heat flux within the bulk. Therefore Eq. (1) and (2) become Eq. (3) and (4), respectively.

$$\left(\rho c_p\right)_{eq} \frac{\partial T}{\partial t} = \nabla \cdot \left(\lambda_{eq} \nabla T\right) + \nabla \cdot \left(L_v \left(\frac{D_{av}}{RT\mu}\right) \nabla (\varphi p_{sat})\right) - \left(\rho c_p\right)_{eq} u \cdot \nabla T \tag{3}$$

$$\frac{\partial w}{\partial t} = -\nabla \cdot \left(-\frac{D_{av}}{RT\mu} \nabla (\varphi p_{sat})\right) - u \cdot \nabla w \tag{4}$$

A third additional momentum equation would be therefore necessary to study the velocity field and the associated heat and mass fluxes. In order to simplify the problem, in the heat transfer equation the convective contribution can be included in the conductive term. This combined effect of conduction and convection is expressed through the Nusselt number (*Nu*), the ratio of convection to pure conduction [17]:

$$h = \frac{Nu\lambda}{\Delta x} \tag{5}$$

Equation (3) can therefore be expressed using an effective thermal conductivity value ($\lambda \bullet Nu$), which considers the combined effect of conductive and convective heat transfer [18]. The investigation of the role played by natural convection in this application is important to evaluate the actual performance of the material. If the Nusselt number approaches the unity, convection has a negligible influence on the total heat transfer, and thermal conduction is the most relevant heat transfer mechanism.

For what concerns the moisture transport (Eq. (4)), a similar approach can be used. The contribution of the buoyancy forces on the concentration gradients can be expressed in the diffusive term of Eq. (4), using an effective water vapor resistance factor (μ_{eff}), defined as a function of the Sherwood number (Eq. (7)) [17].

$$\mu_{eff} = \frac{\mu}{Sh} \tag{6}$$

$$Sh = \frac{h_m L}{D_{AV}} \tag{7}$$

Both Nusselt and Sherwood numbers can be derived as a function of the Rayleigh number, which gives an indication of the strength of the fluid flow and which in the Darcy-modified form can be applied to porous materials [18]. The Darcy-modified Rayleigh number depends on the temperature difference, the specimen thickness, permeability and thermal conductivity and the fluid characteristics [19, 20].

With the mentioned simplifications, the momentum equation is not anymore needed and the numerical simulations can be carried out with a significantly lower computational effort using Eq. (8) and (9).

$$\left(\rho c_p\right)_{eq} \frac{\partial T}{\partial t} = \nabla \cdot (\lambda \cdot Nu \nabla T) + \nabla \cdot \left(L_v \left(\frac{D_{av}}{RT \frac{\mu}{Sh}} \right) \nabla (\varphi p_{sat}) \right) \tag{8}$$

$$\frac{\partial w}{\partial t} = -\nabla \cdot \left(-\frac{D_{av}}{RT \frac{\mu}{Sh}} \nabla (\varphi p_{sat}) \right) \tag{9}$$

5 Numerical Model of TES Cover

A finite-element model of one section of the cover is created using the software COMSOL Multiphysics and used to run a series of parametric studies to investigate the impact of two parameters: one geometrical-related (i.e. the ventilation pipes distance, see Fig. 1b) and one material-related (the moisture diffusion resistance factor μ). Since the goal is to study the optimal design of the ventilation pipes in a well performing insulation, the convection within the porous insulation is neglected and therefore the water vapor resistance factor is assumed to be always larger than 1, while the Nusselt number could be assumed equal to 1 (see Eq. (8) and (9)). Figure 1b presents a sketch of the design with the implemented boundary conditions, while Table 1 lists the relevant parameters used in the simulation.

Table 1. Insulation material properties used in the simulation [10].

Insulation material (i.e. FGG)		
Thermal conductivity, λ	0.1	[W/(m•K)]
density, ρ	180	[kg/m^3]
heat capacity, c_p	1000	[J/(kg•K)]
Free saturation water content, u_{fs}	300	[kg/m^3]

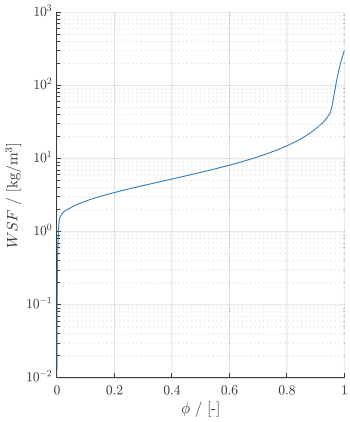

Fig. 2. TES cover insulation water storage function (WSF).

Since no data were available for the FGG moisture retention curve, the shape of the desorption curves available in literature [21] was used and scaled to the free saturation water content of the FGG [10]. The resulting water storage function (WSF) used to run the simulation is presented in Fig. 2.

In order to gain a comprehensive overview of the role of ventilation pipes, their distance (d) was varied between 0.2 and 0.6 m (see Fig. 1b) with a water vapor resistance factor μ ranging between 1 and 10. The cover is in contact with the TES upper water layers at 60 °C and with the ambient air at 10 °C. The initial relative humidity inside the insulation is 90% (corresponding to an initial water mass of 25.6 kg/m^3), while the surrounding ambient humidity is 10%. Both upper and bottom liners are assumed impermeable; therefore the remaining construction moisture can only be removed through the ventilation pipe. A simulation period of 30 days is considered.

6 Experimental Set-Up

In order to answer the questions concerning the actual FGG performance in presence of construction moisture in the TES cover, a mock-up is set up in the climate chamber of the Unit of Energy Efficient Building of the University of Innsbruck. The mock-up consists of a (1x1x0.5) m open steel case filled with loose FGG. In order to simulate the operation conditions that can be encountered in a TES cover, a heating plate is placed under the lower side of the case to ensure a constant set point temperature. The lateral surface of the steel case is insulated to simulate adiabatic conditions.

Aim of the test is the evaluation of the impact of convection on the total heat transfer in presence of high temperature differences and the definition of the time required for the complete evaporation of the water to achieve a condition of dry substrate. In order to measure the gradual weight loss caused by the water evaporation, each container is placed on a balance (with a readability of 5 g). A parallel measurement of the thermal conductivity of the FGG is conducted; at this purpose, a guarded hot plate is installed, in order to prevent downward heat loss from the heat source and to attain unidirectional

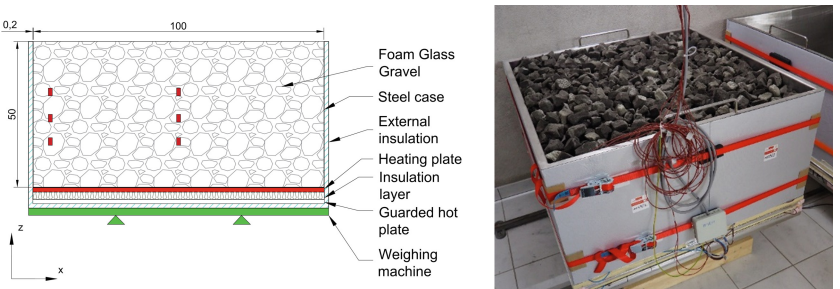

(a) (b)

Fig. 3. (a) Schematic side view of TES cover mock up (measures in [cm]) and (b) actually realized mock up.

Table 2. Characteristics of the investigated FGG samples.

	Sample 1	Sample 2	Sample 3	Sample 4
% compaction	0 (uncompacted)	10%	20%	30%
ρ / [kg/m^3]	140	160	180	190
ψ porosity	0.32	0.28	0.24	0.2

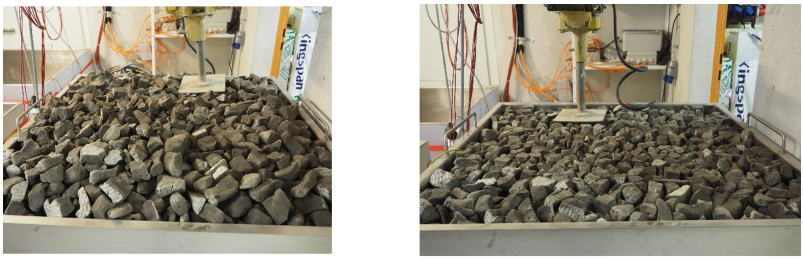

(a) (b)

Fig. 4. The desired compaction degree was achieved in three compression steps, in order to ensure an homogenous compaction. The photos show the last step (a) before and (b) after the compaction (Sample 4).

upwards heat flow. Additionally, six temperature sensors (PT100) per each container are installed with the distribution presented in Fig. 3a: three sensors are installed in the central part of the FGG domain and 3 near the container's border. Two additional sensors are placed on the heating plates in order to monitor the imposed boundary conditions.

Four mock-ups, whose characteristics are presented in Table 2, are realised to gain a detailed overview of the behaviour of FGG under different compaction degrees. The desired degree of compaction (in samples 2, 3 and 4) is obtained with three compaction steps in order to achieve a homogeneous domain (see Fig. 4).

6.1 Methodology

The first part of the test consisted in the evaluation of the effective thermal conductivity of the material in dry conditions. The hot plate temperature is set to 60 °C while the climate chamber is kept at a constant temperature of 20 °C. A reference test using rockwool (RW) is used to calibrate the tests in dry conditions. A 2D numerical model of the set-up is realised using a finite element-modelling tool (COMSOL Multiphysics).

The second part of the test consists in the addition of a predefined amount of water to each container with FGG and the measurement of the time required for its complete evaporation with the pre-defined hot plate set point temperature. In contrast to the previous test in dry conditions, where a steady state behaviour could be observed after a pre-heating phase, the gradually evaporating water leads to transient conditions.

Considering the reference provided by the measurements and using the Nusselt values defined from the dry tests, it is possible to evaluate the effective water vapour diffusion resistance factor for the FGG with different compaction.

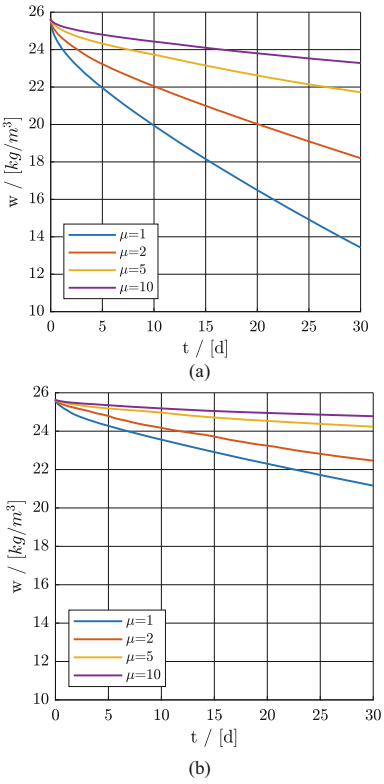

Fig. 5. Resulting cumulative water loss for the analysed cases. (a) d = 0.2 m. (b) d = 0.6 m.

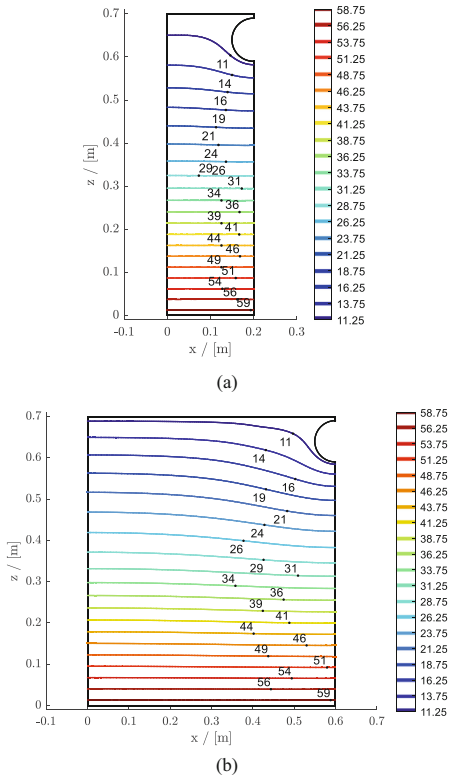

Fig. 6. Temperature distribution inside the insulation at the end of the 30 days for the case with $\mu = 1$. (a) d = 0.2 m. (b) d = 0.6 m.

6.2 Results and Discussion

6.2.1 TES Cover Numerical Model

The resulting drying curves are presented in Fig. 5. The high temperature of the cover close to the TES water contributes in gradually removing the local moisture (see Fig. 6). It is possible to see that the use of closer pipes allows a more rapid removal of the trapped moisture, but the insulation material properties and installation have a deep impact in terms of water vapor resistance (see Fig. 7).

Therefore, a highly permeable bulk insulation (i.e. with low μ) is desirable since it allows a faster removal of the eventually present moisture, thus facilitating the installation works and ensuring a higher insulation performance.

6.2.2 Experimental Set-Up: Dry Conditions

From the tests in dry conditions it has been possible to define the Nusselt number (Eq. (5)), that quantifies the influence of natural convection in that configuration. A first round of test and simulations is run for the reference case (with RW) to consider the impact of the set-up (i.e. lateral losses and influence of stainless steel). The RW declared nominal

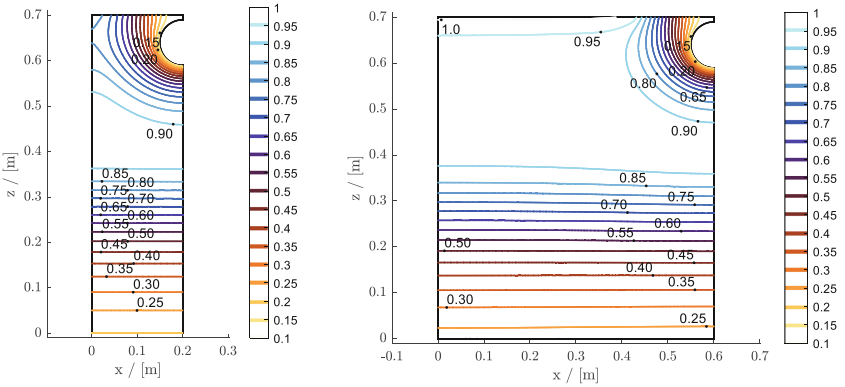

Fig. 7. Relative humidity inside the insulation at the end of the 30 days for the case with $\mu = 1$. (a) d = 0.2 m. (b) d = 0.6 m.

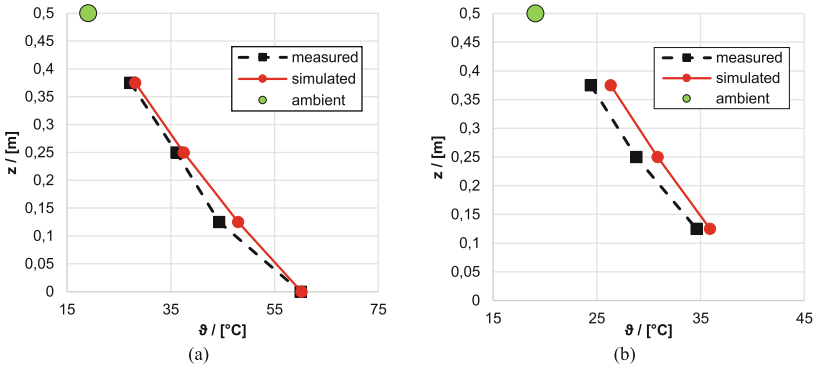

Fig. 8. Measured and simulated vertical temperature profiles in the RW during the reference measurement (hot plate at 60 °C). (a) Central sensors. (b) Side sensors

thermal conductivity at 60 °C is 0.05 W/(m•K) according to the producer's datasheet; the high declared equivalent air layer thickness (>200 m) supports the assumption that the development of convective heat flux can be negligible. However, in the experimental set up a thermal conductivity value of 0.06 W/(m•K) is reached, which is justified by the specimen thickness (50 cm) and the high temperature difference (40 K), that deviate from the nominal boundary conditions of the datasheet. The comparison of the simulated and measured temperatures is presented in Fig. 8 (the small discrepancy is linked to the error of the sensors and to their eventual position shifts during the installation).

For the FGG evaluation, the comparison between the simulated and measured temperature values for different Nusselt numbers is presented in Fig. 9. In sample 1 (uncompacted FGG) the high instability of the temperature measured by the sensors in the bulk suggests that the developed natural convection does not allow to reach a steady state, therefore the time average temperature values are used (Fig. 9a) [22]. When looking at

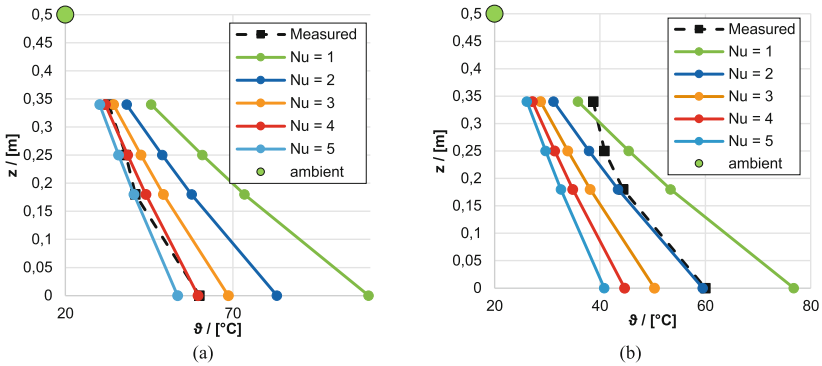

Fig. 9. Comparison of the simulated and measured temperatures in the central section during the test with hot plate temperature of 60 °C. (a) Sample 1: uncompacted FGG (b) Sample 4: comp. 30%.

the compacted FGG (Fig. 9b), it is possible to observe that increasing the compaction degree (i.e. higher densities) a more stable temperature profile is reached, and the Nusselt number drops, meaning that the convective transfer is reduced. Yet, the influence of convection remains significant, since the final thermal conductivity for a compaction of 30% ($\rho = 190$ kg/m^3) is still higher than the nominal value (Nu = 1).

As can be inferred from Fig. 9, the average Nusselt number that can be estimated from the analysis is ca. 4 for the uncompacted FGG and ca. 2 for the 30% compacted FGG. Yet, it is important to mention that this value is strongly dependent on the local temperature and local compaction degree (that could be inhomogeneous along the volume of the specimen), as well as on the bulk layer thickness. Compared to the reference case with the RW, where the convection is minimized, a significant temperature drop is observed proceeding towards the side of the container. This is related to the presence of the buoyant plume, which results in the upward flow of the high temperature air in the central part of the specimen and in the downward flow of the colder ambient air along the borders [22].

6.2.3 Experimental Set-Up: Presence of Moisture

With the Nusselt values derived in the dry test, it is then possible to estimate the effective vapor diffusion resistance factor (μ_{eff}) in presence of moisture. The hot plates temperature are set to 60 °C and, after the four samples reached steady-state conditions, a total amount of 10 l of water is sprayed on each container.

Figure 10 shows the resulting cumulative curves of the evaporated water from the four samples. It is possible to observe that the containers with higher FGG compression degree required longer time for a complete dry out. The reason can be found in their lower porous fraction, which does not only reduce the convective heat transfer, as previously observed in dry conditions in Fig. 9, but also the convective moisture transport (see Eq. (4)).

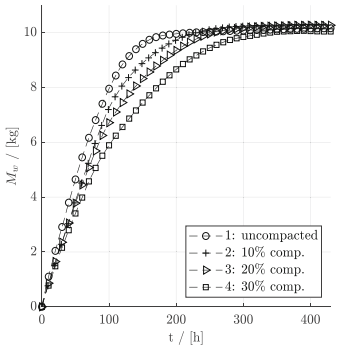

Fig. 10. Cumulative curve of the evaporated water amount. (a) hot plate temperature 60 °C, 10 l of water.

From the numerical simulations it is then possible to define the values of μ_{eff}, for the given FGG configurations. Equation (8) and (9) are implemented in COMSOL Multiphysics using the "Heat Transfer" and "Moisture Transport in Building Materials" modules with the imposed boundary conditions (ambient temperature and input power) and the given initial water content.

The curves resulting from the simulations are then compared to the measured values. Thus, Fig. 11 shows the comparison between the measured (black dashed lines) and simulated values (continuous lines) for samples 1 (uncompacted FGG) and 4 (30% comp. FGG). The curve with $\mu_{eff} = 1$ is introduced since it represents the water vapor resistance produced by an air layer, and can be used as reference value. It is possible to see that the loose material (Fig. 11a) exhibits the lowest value of water vapor resistance ($\mu_{eff} = 0.1$ to 0.2), while the compacted one (Fig. 11b) shows slightly higher values (μ_{eff} in the range of 0.3). Values of effective water vapor resistance lower than 1 are attributable to the convective component, which is included in $\mu_{eff,}$ and determines the enhanced transport mechanism with respect to a condition where ($\mu_{eff} = 1$), meaning that the drying of the material is primarily driven by convection than diffusion [19].

7 Conclusions and Outlook

In the present study the main parameters affecting the TES cover performance were investigated under the operation conditions of a TES. Convection and moisture penetration were in this perspective studied as the main source of insulation degradation in bulk materials.

From the numerical simulations, the installation of ventilation pipes to remove eventually trapped moisture appears to be an effective solution, given the appropriate knowledge of the material properties (i.e. water vapor resistance factor). However, in presence of such high temperatures and bulk thicknesses, convection is not a negligible factor.

The compaction of FGG plays an important role in its final insulation performance. From the conducted tests in dry conditions it is possible to see that compaction contributes on the blocking of convective heat transfer, resulting in lowers value of effective thermal conductivity. Yet, considering the case of upward heat flux (as in a TES cover) and

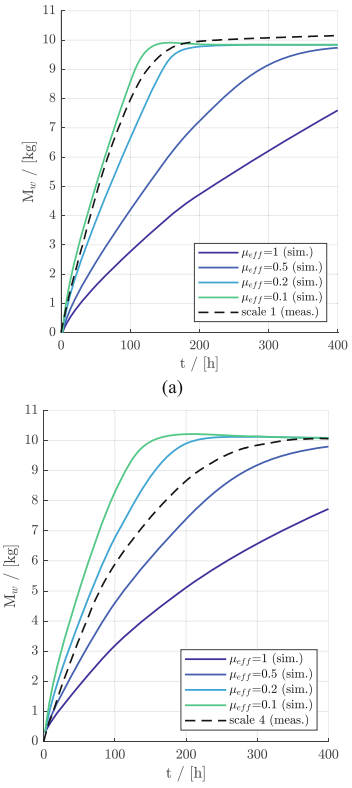

Fig. 11. Comparison between measured and simulated cumulative curves of evaporated water. (a) loose FGG (sample 1), (b) 30% comp. FGG (sample 4).

the high temperature differences involved, the final measured insulation performance of ca. 0.2 W/(m•K) may not be acceptable, considering that the nominal value of FGG is 0.1 W/(m•K).

When considering the presence of moisture, it is possible to see that the mass transport related to convection is much more relevant than the one related to diffusion, since the resulting effective water vapor resistance factors are lower than 1 (see Fig. 11). The presence of convection contributes to a faster removal of the eventually present construction moisture, thanks also to the high temperature gradient within the insulating bulk. While the corresponding measures that can be taken to tackle these problems appear to be conflicting, the study showed that an appropriate knowledge of the material properties is one of the keys for a well performing TES cover.

This study serves as a basis for investigating possible solutions to be implemented to further reduce the convection, still enabling the removal of moisture. In the investigated case, bulk compaction improves the insulation performance with respect to the uncompacted case, but it may not be sufficient to block convection, given the large bulk thickness and high temperature differences. Moreover, a high compaction degree would require a larger amount of material and a further increase of the installation works. Convection brakes can effectively reduce the buoyant plume and the consequent velocity field that drives convection, but must be designed and installed to allow the eventual water vapor transfer in case of residual construction moisture. Moreover, the vertical interval between the brakes must be carefully designed according to the velocity field that develops within the bulk, which depends on the material itself. The minimisation of porosity and thus of convection can also be achieved using insulation materials with wider granulometric range or by mixing materials with different granules sizes.

It is important to remark that removing construction moisture and minimising convection alone will not solve the problem of the poor insulation performance, if moisture diffusion will occur from the TES through the liner.

Given the knowledge available from the material tests, it is now important to develop proper design solutions for the TES envelope component. In particular, it is important to remark that the appropriate selection of the insulation material and its properties cannot disregard location and role of the specific component in order to achieve the design insulation performance.

The implementation of simulation tools to support design of robust TES cover is a valid help but it must be based on reliable insulation material properties, i.e. the actual performance of the material under real TES conditions.

Acknowledgments. This research was carried within the framework of IEA ECES Annex 39 ("Großwärmespeicher für Fernwärmesysteme") and the Austrian flagship research project "Giga-Scale Thermal Energy Storage for Renewable Districts" (giga_TES, Project Nr.: 860949), financed by the Austrian "Klima- und Energiefonds". Therefore, the authors wish to acknowledge the financial support for this work.

Nomenclature.

Symbol	Description
Latin Symbols	
c_p	specific heat capacity / [J/(kg•K)]
D_{av}	vapour diffusivity in air/ [m^2/s]
h	heat transfer coefficient / [W/(m^2•K)]
h_m	convection mass transfer coefficient / [m/s]
L	length / [m]
L_v	latent heat / [J/kg]
M	mass / [kg]

(*continued*)

(*continued*)

Symbol	Description
p	pressure / [Pa]
R	gas constant / [J/(kg●K)]
T	temperature / [K]
t	time / [s]
u	velocity / [m/s]
w	specific water content / [kg/m^3]
x	horizontal coordinate / [m]
z	vertical coordinate / [m]
ϑ	temperature / [°C]
λ	thermal conductivity / [W/(m●K)]
μ	water vapour diffusion resistance factor / [-]
ρ	density / [kg/m^3]
φ	relative humidity / [-]
Subscripts	
a	air
eff	effective
ins	insulation
m	mass
sat	saturation
V	vapour

References

1. M. Kaltschmitt, W. Streicher, and A. Wiese, Erneuerbare Energien, Systemtechnik - Wirtschaftlichkeit - Umweltaspekte. Springer-Verlag, 2020
2. R. Roseen and B. Perers, "A Solar Heating Plant in Studsvik: Design and First-year Operational Performance," Lulea (Sweden), 1980.
3. D. Tschopp, Z. Tian, M. Berberich, J. Fan, B. Perers, and S. Furbo, "Large-scale solar thermal systems in leading countries: A review and comparative study of Denmark, China, Germany and Austria," Applied Energy, vol. 270. Elsevier Ltd, p. 114997, Jul. 15, 2020, doi: https://doi.org/10.1016/j.apenergy.2020.114997.
4. P. A. Sørensen et al., "Follow-up on large scale heat storages in Denmark," 2019.
5. I. Sifnaios, A. R. Jensen, S. Furbo, and J. Fan, "Performance comparison of two water pit thermal energy storage (PTES) systems using energy, exergy, and stratification indicators," J. Energy Storage, vol. 52, p. 104947, Aug. 2022, doi: https://doi.org/10.1016/J.EST.2022.104947.

6. W. van Helden et al., “Giga-scale thermal energy storage for renewable districts - Publishable final report,” 2021. [Online]. Available: https://www.gigates.at/index.php/en/publications/reports.
7. P. A. Sørensen and T. Schmidt, “Design and Construction of Large Scale Heat Storages for District Heating in Denmark,” 2018.
8. A. Tosatto, F. Ochs, A. Dahash, C. Muser, F. Kutscha-Lissberg, and P. Kremnitzer, “Insulating piles for the cost-effective construction of very large-scale high temperature thermal energy storage,” in Proceedings of the International Renewable Energy Storage Conference 2021 (IRES 2021), 2022, no. Atlantis Highlights in Engineering, pp. 67–77, doi: https://doi.org/10.2991/ahe.k.220301.007.
9. M. Grabmann, G. Wallner, K. Grabmayer, W. Buchberger, and D. Nitsche, “Effect of thickness and temperature on the global aging behavior of polypropylene random copolymers for seasonal thermal energy storages,” Sol. Energy, vol. 172, pp. 152–157, Sep. 2018, doi: https://doi.org/10.1016/J.SOLENER.2018.05.080.
10. F. Ochs, “Modelling Large-Scale Thermal Energy Stores,” University of Stuttgart, 2009.
11. A. Tosatto, F. Ochs, A. Dahash, and C. Muser, “The Challenge of Planning and Constructing Large-Scale Hot Water TES for District Heating System : A Techno-Economic Analysis,” in Proceedings of the International Renewable Energy Storage Conference 2021 (IRES 2021), 2022, vol. 8, no. Atlantis Highlights in Engineering, pp. 52–66, doi: https://doi.org/10.2991/ahe.k.220301.006.
12. A. Dahash, F. Ochs, A. Tosatto, and W. Streicher, “Toward efficient numerical modeling and analysis of large-scale thermal energy storage for renewable district heating,” Appl. Energy, vol. 279, 2020, doi: https://doi.org/10.1016/j.apenergy.2020.115840.
13. A. Dahash, F. Ochs, and A. Tosatto, “Techno-economic and exergy analysis of tank and pit thermal energy storage for renewables district heating systems,” Renew. Energy, vol. 180, pp. 1358–1379, Dec. 2021, doi: https://doi.org/10.1016/J.RENENE.2021.08.106.
14. A. Dahash, F. Ochs, G. Giuliani, and A. Tosatto, “Understanding the interaction between groundwater and large-scale underground hot-water tanks and pits,” Sustain. Cities Soc., vol. 71, p. 102928, Aug. 2021, doi: https://doi.org/10.1016/j.scs.2021.102928.
15. International Energy Agency (IEA), “SHC Task 45 Large System Seasonal thermal energy storage - Report on state of the art and necessary further R + D,” Stuttgart (Germany), 2015. [Online]. Available: http://task45.iea-shc.org/data/sites/1/publications/IEA_SHC_Task45_B_Report.pdf.
16. M. Bianchi Janetti, T. Plaz, F. Ochs, O. Klesnil, and W. Feist, “Thermal conductivity of foam glass gravels: A comparison between experimental data and numerical results,” in 6th Int. Build. Phys. Conf. IBPC 2015, Torino, Italy, 2015, vol. 78, pp. 3258–3263, doi: https://doi.org/10.1016/j.egypro.2015.11.713.
17. F. P. Incropera, D. P. Dewitt, T. L. Bergman, and A. S. Lavine, Incropera’s Principles of Heat and Mass Transfer, Global Edi. Wiley, 2017.
18. VDI-Wärmeatlas, 10th ed. Springer Verlag, 2006.
19. M. Bianchi Janetti, “Hygrothermal Analysis of Building Components Inclosing Air Cavities : Comparison between Different Modeling Approaches and Experimental Results,” University of Innsbruck, 2015.
20. H. D. Baehr and K. Stephan, Heat and Mass Transfer, 3rd ed. 2011.

21. M. Bianchi Janetti, L. P. M. Colombo, F. Ochs, and W. Feist, “Effect of evaporation cooling on drying capillary active building materials,” Energy Build., vol. 166, 2018, doi: https://doi.org/10.1016/j.enbuild.2017.12.048.
22. F. Ochs, M. Bianchi Janetti, Ondrej Klesnil, “Wärmeleitfähigkeit von Schüttungen aus Glasschaumgranulat: Messtechnische Analyse sowie Analytische und Numerische Modellierung,” 2015. [Online]. Available: http://www.aee-now.at/cms/fileadmin/downloads/projekte/store4grid/store4Grid Wärmeleitfähigkeit.pdf.